Electron Affinity of Strontium

D. Berkovits,[1] E. Boaretto,[1] S. Ghelberg,[1] O. Heber,[2] and M. Paul[1]
[1]*Racah Institute of Physics, Hebrew University, Jerusalem, Israel 91904*
[2]*Accelerator Laboratory, Weizmann Institute, Rehovot, Israel 76100*
(Received 4 January 1995)

We have observed a threshold in the electron photodetachment cross section of $^{88}Sr^-$ ions at a photon energy $h\nu = 1.820$ eV and assign it to a p-wave transition from the $5s^25p\,^2P$ ground state in Sr^- to the $5s5p\,^3P$ state in neutral Sr. The measurement was made with a new technique combining the tunable laser photodetachment threshold method with accelerator mass spectrometry. We determine for the first time the electron affinity of Sr to be 48 ± 6 meV, much smaller than predicted in recent calculations. The $^2P_{1/2}$-$^2P_{3/2}$ fine splitting of the Sr^- ground state is estimated to be 26 ± 8 meV.

PACS numbers: 32.10.Hq, 07.75.+h, 32.80.Fb

Investigations of the stability of free negative ions provide excellent testing grounds for our understanding of the many-body problems of electrons bound to nuclei and the subtle electron correlation processes. The case of Ca^-, in particular, has become fascinating when, in contrast to former predictions, it was experimentally discovered to form a stable negative ion [1]. Confirmed by calculations, this state is described as a $4p$ electron bound to the Ca ground state to form a $4s^24p\,^2P$ configuration [2]. The electron affinity was then predicted to be 45 meV [2] (see also [3,4] for recent references) and measured as 43 ± 7 meV [1]. Later experiments [5–9], however, have converged to a much smaller value of 18.4 ± 2.5 meV [6]. At the same time, many theoretical studies have tried to improve the precision of calculations [3] and to include polarization effects in inner electronic shells (core polarization) [10,11]. The demand on these calculations is indeed stringent, since the binding energy of the outermost electron is very small compared to that of the total electronic energy of the atom (~18 keV). Properties of negative ions of heavier alkaline earths are as yet largely unknown experimentally, but several calculations have recently been published [10,12–18] and predict stable negative ions to be formed when a np electron attachs itself to the ground state neutral atom. We present here the first experimental determination of the electron affinity of Sr using a new technique combining the laser photodetachment threshold (LPT) method with an accelerator mass spectrometer. Our measured value of 48 ± 6 meV differs markedly from the above theoretical predictions, most of which are around or above 100 meV. This situation is similar to the aforementioned case of Ca^-, indicating that the discrepancy between theory and experiment has a physical source. It is possible that for Sr^- also the inclusion of core polarization (see, for instance, Ref. [10]) can lead to a significant decrease in the calculated values of the electron affinity and brings them into better agreement with the measured value.

The experimental study of Sr^- is hampered by a weak negative ion yield. Although a stable or perhaps metastable state of Sr^- was shown to exist [19] and the electron affinity estimated to $\lesssim$0.1 eV [20], no precise determination was made prior to the present work. We have used here the LPT method in combination with accelerator mass spectrometry (AMS) [21–23] for the unambiguous identification of Sr^-. Our experimental system (Fig. 1) includes a high-intensity Cs-sputter negative ion source (GIC 860) loaded with a freshly cut metallic Sr (99%) cathode. Sr^- ions are directly extracted, magnetically deflected, and preaccelerated to an energy of 115 keV. The ion beam is electrostatically focused into a 1 m long region (at ~2×10^{-7} Torr) where it interacts with a pulsed dye laser beam (pulse duration ~10 ns) in an antiparallel configuration. The dye laser (Quantel TDL-50) is pumped by a frequency-doubled Q-switched Nd-YAG laser (Quantel YG-581-30). The defining (retractable) apertures at each end of the interaction region are 3 mm in diameter, collimating both the ion and photon beams. The

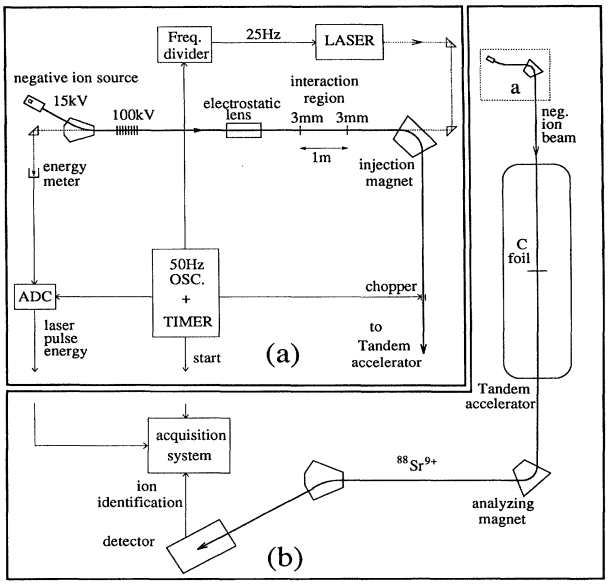

FIG. 1. Schematic diagram of the experimental setup.

 0031-9007/95/75(3)/414(4)$06.00

energy of individual laser pulses is measured by use of a calibrated energy meter situated outside the vacuum vessel [see Fig. 1(a)], and the signal is fed after digitization into the data acquisition computer. In most measurements, the pulse energy (corrected for absorption in windows and prisms) averaged 60 μJ with a standard deviation of about 20 μJ. A correction to the geometrical flux through the apertures was applied in order to derive an effective flux which includes the effect of ion beam focusing [24]. Neutral atoms resulting from photodetachment in the laser light are eliminated from the ion beam after a 90° magnetic analysis ($m/\Delta m = 235$). The ion beam is electrostatically chopped into 2.7 μs long pulses with a timing such that only ions, which were in the interaction region at the time of laser firing, are transmitted. Residual negative ions are injected for identification into a tandem electrostatic accelerator (NEC 14UD Pelletron) used as an accelerator mass spectrometer [24,25]. After acceleration by a terminal voltage around +10 MV, the ions are stripped in a thin C foil, further accelerated, analyzed as $^{88}Sr^{9+}$ ions at an energy of 97.97 MeV, and transported to a nuclear particle detector system. The crucial role of the AMS analysis lies in the identification of individual ions reaching the detector. These ions are counted after acceleration with unit efficiency and kinetic energy (E) and time of flight (TOF) are measured. The ion identification is especially important when sputter sources are used. This type of source is versatile and able to efficiently produce any negative ion species but also generate intense background beams of atomic and molecular ions.

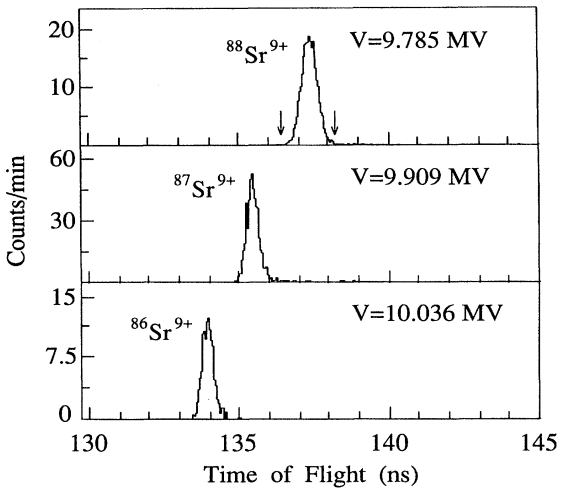

FIG. 2. Time-of-flight spectra measured in the particle detector for different accelerating voltages V at the *same* setting ($M = 88$) of the injection mass analyzer. ^{88}Sr ions are injected as $^{88}Sr^-$ while the ^{87}Sr and ^{86}Sr ions result from dissociation of $^{87}SrH^-$ and $^{86}SrH_2^-$ molecular ions, respectively, in the tandem stripper foil. The spectra were measured with an attenuated beam and without the chopper. The arrows show the TOF channel limits used to gate on ^{88}Sr ions.

This is illustrated for our experiment in Fig. 2, where the presence of the hydride molecular ions $^{87}SrH^-$ and $^{86}SrH_2^-$ in the mass-analyzed beam ($M = 88$) is shown. After dissociation of the molecules in the stripper foil, the ^{87}Sr and ^{86}Sr fragments are separated from the ^{88}Sr ions by the high-energy 90° magnet. The intensity of the elemental $^{88}Sr^-$ component was estimated to be only 5.2% of the total mass-analyzed $M = 88$ negative ion beam intensity (~40 pA). All measurements discussed below were taken at the accelerating voltage corresponding to transmission of ^{88}Sr and, furthermore, the Sr ions were counted by applying a software gate on TOF channels corresponding to ^{88}Sr ions (see Fig. 2). In order to study the interaction between negative ions and photons, we measure the spectrum of arrival times at the detector (t_a) of ions having survived the laser interaction, using the opening time of the chopper as a start signal. The t_a spectrum represents the intensity of the $^{88}Sr^-$ ion beam as a function of time (or distance) along the interaction region and the laser-depleted ion counts are determined by the integral n of the t_a spectrum in this region. We measure the transmission ratio T of the ion beam through the laser pulse as the ratio n/n_0 of ions accumulated in t_a spectra, alternately with and without laser. To obtain these two spectra, the ion beam is chopped at twice the laser repetition rate, so that every second ion pulse is transmitted without laser interaction. Effects of ion losses through the spectrometer or negative ion neutralization by collisions in the residual gas are canceled in this ratio. Pileup of particle signals which may occur when more than one particle per ion pulse reaches the detector is taken into account in the analysis. The setup, detector, and analysis scheme are described in more detail in [24–26].

Photon wavelengths (615 to 711 nm) were selected close to the threshold value expected for the transition leaving the neutral Sr atom in its first excited configuration $5s5p\,^3P$. The dependence of the measured transmission ratio T on the photon energy (Doppler corrected), shown in Fig. 3(a), displays a clear threshold for $h\nu \sim 1.820$ eV; the transmission then levels off around 1.9 eV. In the conditions of our experiment, the dependence of T on the photon fluence ϕ was nearly exponential and the photodetachment interaction can be expressed by an effective cross section σ related to the transmission ratio by $T = e^{-\sigma\phi}$. The cross section determined in this way is shown in Fig. 3(b) in the region of the threshold; the uncertainty on the cross section scale is estimated to be 25%. The shape of the curve is very similar to that measured by Walter and Peterson [5,6] for the transition $4s^24p\,^2P$ Ca^- to the $4s4p\,^3P$ Ca^0 excited configuration. We notice that the production of negative ions by sputtering and direct extraction precludes significant population of possible excited (metastable) states of Sr^- and interpret the threshold as a p-wave detachment from the ground state negative ion, assumed to be $5s^25p\,^2P$ as predicted by calculations. A pure p-wave assignment is also supported by the fact

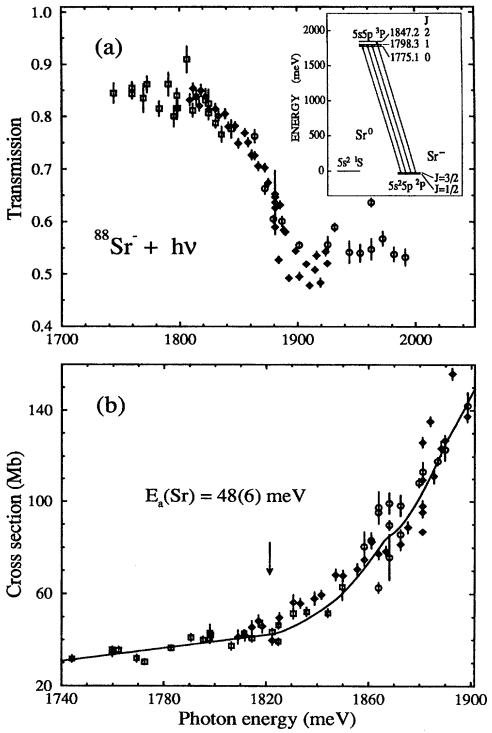

FIG. 3. (a) Transmission ratio of the $^{88}Sr^-$ beam through the dye laser pulse (integrated for photon fluences between 2.5×10^{15} and 6.5×10^{15} photons/cm^2) in the measured photon energy range. The symbols correspond to the different dyes used to cover this range: ○, DCM; ◇, DCM + LDS698; □, LDS698. The error bars represent the statistical errors on ion counting. The inset shows the expected fine splitting of the Sr^- ground state and of the final state in Sr, their excitation energy, and the allowed transitions. (b) Effective cross section of electron photodetachment for $^{88}Sr^-$ ions in the region of the threshold of the $5s^25p\,^2P$ $Sr^- \rightarrow 5s5p\,^3P$ Sr^0 transition. The line is calculated from the results of a best fit by Eqs. (1) and (2) (see text). The arrow indicates the value of the Sr electron affinity extracted from the fit. Note that due to the fortuitous relation $E_{fs} \sim E_1 - E_0$ the thresholds of the transitions $J = 1/2 \rightarrow J' = 0$ and $J = 3/2 \rightarrow J' = 1$ nearly coincide.

that any s-wave component in the transition would involve parity violation. The cross section as a function of photon energy $h\nu$ above and near a threshold is expected to follow the Wigner relation [27,28] $\sigma \propto (h\nu - E_0)^{(l+1/2)}$, where E_0 is the threshold energy and l the angular momentum of the outgoing particle ($l = 1$), superimposed on a background representing transitions to the neutral Sr ground state. The background is approximated here as a linear function of photon energy. The fine-structure splitting $^2P_{1/2}$-$^2P_{3/2}$ expected in the Sr^- ground state (see Fig. 3, inset) must, however, be taken into account to interpret our results. The value of the splitting in Sr^- has been predicted as 22 [17] and 28 meV [18], and it is believed that the precision in this calculation is much better than in the absolute energy of the negative ion ground state. Both levels are expected to be populated, assuming a Boltzmann distribution at an electronic temperature $T_{el} = 1500$ K which is typical in Cs-sputter ion sources [29]. When the photodetachment channels from both levels are energetically open, the depletion of the ion beam is due to two distinct cross sections. We analyze therefore the set of data for the transmission $T = T(\phi, h\nu)$ up to $h\nu \sim 1.93$ eV (about 900 points), using the following expression:

$$T = \frac{e^{-\sigma_{1/2}\phi} + 2e^{-E_{fs}/kT_{el}}e^{-\sigma_{3/2}\phi}}{1 + 2e^{-E_{fs}/kT_{el}}}, \qquad (1)$$

where E_{fs} is the fine-structure splitting energy. The individual cross sections $\sigma_{1/2}$ and $\sigma_{3/2}$ are then expressed as described above by

$$\sigma_J = \sigma_0 + ah\nu + bh\nu \sum_{J'} W_{JJ'}(h\nu - E_{J'} - E_{a_J})^{3/2}. \qquad (2)$$

In this equation,

$$W_{JJ'} = (2J' + 1)\begin{Bmatrix} S & J & L \\ J' & S' & \frac{1}{2} \end{Bmatrix}^2$$

is the statistical and geometrical coefficient under assumption of L-S coupling derived from [30] (see also [1,28,31]) for the transition from state $J = 1/2, 3/2$, $L = 1$, $S = \frac{1}{2}$ in ^2P_J Sr^- to state $J' = 0, 1, 2$, $L' = 1$, $S' = 1$ in $^3P_{J'}$ Sr. $E_{J'}$ is the spectroscopically determined excitation energy (see Fig. 3, inset [32]) for this state J' and E_{a_J} the electron affinity of Sr in state J. The statistical weights $(2J + 1)$ of the initial states are included in Eq. (1) and do not appear in $W_{JJ'}$. An overall least-squares fit of Eqs. (1) and (2) to the experimental values of $T(\phi, h\nu)$ converges well, and we derive the value $E_{a_{1/2}} = 48 \pm 6$ meV. The values obtained for E_{fs} are in the range 26 ± 8 meV. The error bars (1 standard deviation) are estimated from the uncertainty of the fit and the distribution obtained in a large number of fits ($\sim$1600) using different starting values of the fit parameters. We notice that the range of validity of Wigner's law within which Eq. (1) is applied affects the best-fit values of E_a and E_{fs} within the quoted uncertainties. From the present data, this range is estimated to be 45 ± 10 meV. The effective cross section σ_{eff}, calculated using the best-fit values in Eqs. (1) and (2) and the expression $T = e^{-\sigma_{eff}\phi}$, is compared in Fig. 3(b) to the experimental data. The reasonable agreement supports again the p-wave assignment for the transition.

Table I compares our experimental value to the predictions of recent theoretical works. A compelling resemblance is noted between this table for Sr and Table I in [6] for Ca where also most of the theoretical values overestimate the electron affinity. As pointed out, core-polarization effects [10,11] may be the source of the

TABLE I. Comparison of calculations and experimental values of the electron affinity of Sr.

	Ref.	Electron affinity (meV)	Fine splitting (meV)
	Theoretical		
Vosko *et al.* (1989)	[12]	160	
Froese Fischer (1989)	[13]	106	
Kim and Greene (1989)	[14]	108	
Johnson *et al.* (1989)	[15]	93	
Fuentealba *et al.* (1990)	[10]	44	
Gribakin *et al.* (1990)	[16]	129	
Dzuba *et al.* (1991)	[17]	102	22
Cowan and Wilson (1991)	[18]	98	28
	Experimental		
Wilson (1989)	[20]	$\lesssim 100$	
This work		48 ± 6	26 ± 8

necessary corrections. We believe that the present experimental value of the Sr electron affinity provides a new and strong constraint on such calculations. The combination of the LPT method with accelerator mass spectrometry at high energy used here yields a breakthrough in the study of very weakly formed negative ions. We have shown recently that the technique can be refined and made more sensitive by detecting neutral atoms produced rather than the depleted negative beam. The laser photodetachment interaction is performed in the tandem terminal and neutral products are further identified by AMS and separated from the negative beam after a subsequent foil stripping along the high-energy accelerating tube.

We would like to gratefully acknowledge discussions and work in different stages of the experiment with G. Hollos and W. Kutschera, with G. Korschinek in the framework of a grant from the German-Israel Foundation (GIF), and the help of Y. Kashiv in data taking. This work was supported in part by a grant from the German-Israel Foundation (GIF).

[1] D. J. Pegg, J. S. Thompson, R. N. Compton, and G. D. Alton, Phys. Rev. Lett. **59**, 2267 (1987).
[2] C. F. Fischer, J. B. Lagowski, and S. H. Vosko, Phys. Rev. Lett. **59**, 2263 (1987).
[3] C. F. Fischer and T. Brage, Can. J. Phys. **70**, 1283 (1992), and references therein.
[4] S. J. Buckman and C. W. Clark, Rev. Mod. Phys. **66**, 539 (1994).
[5] J. R. Peterson, Aust. J. Phys. **45**, 293 (1992).
[6] C. W. Walter and J. R. Peterson, Phys. Rev. Lett. **68**, 2281 (1992).
[7] H. K. Haugen, L. H. Andersen, T. Andersen, P. Balling, N. Hertel, P. Hvelplund, and S. P. Möller, Phys. Rev. A **46**, R1 (1992).
[8] M.-J. Nadeau, A. E. Litherland, M. A. Garwan, and X.-L. Zhao, Nucl. Instrum. Methods Phys. Res., Sect. B **92**, 265 (1994).
[9] K. W. McLaughlin and D. W. Duquette, Phys. Rev. Lett. **72**, 1176 (1994).
[10] P. Fuentealba, A. Savin, H. Stoll, and H. Preuss, Phys. Rev. A **41**, 1238 (1990).
[11] H. W. van der Hart, C. Laughlin, and J. E. Hansen, Phys. Rev. Lett. **71**, 1506 (1993).
[12] S. H. Vosko, J. B. Lagowski, and I. L. Mayer, Phys. Rev. A **39**, 446 (1989).
[13] C. F. Fischer, Phys. Rev. A **39**, 963 (1989).
[14] L. Kim and C. H. Greene, J. Phys. B **22**, L175 (1989).
[15] W. R. Johnson, J. Sapirstein, and S. A. Blundell, J. Phys. B **22**, 2341 (1989).
[16] G. F. Gribakin, B. V. Gultsev, V. K. Ivanov, and M. Yu Kuchiev, J. Phys. B **23**, 4505 (1990).
[17] V. A. Dzuba, V. V. Flambaum, G. F. Gribakin, and D. P. Sushkov, Phys. Rev. A **44**, 2823 (1991).
[18] R. D. Cowan and M. Wilson, Phys. Scr. **43**, 244 (1991).
[19] L. R. Kilius, N. Bada, M. A. Garwan, A. E. Litherland, M.-J. Nadeau, J. C. Rucklidge, G. C. Wilson, and X.-L. Zhao, Nucl. Instrum. Methods Phys. Res., Sect. B **52**, 357 (1990).
[20] R. G. Wilson, *Proceedings of the Seventh International Conference on Secondary Ion Mass Spectrometry, SIMS VII, California, 1989* (Wiley, New York, 1990), p. 131.
[21] A. E. Litherland, Ann. Rev. Nucl. Part. Sci. **30**, 437 (1980).
[22] W. Kutschera and M. Paul, Ann. Rev. Nucl. Part. Sci. **40**, 411 (1990).
[23] M. Paul, Nucl. Instrum. Methods Phys. Res., Sect. A **328**, 330 (1993).
[24] D. Berkovits, E. Boaretto, G. Hollos, W. Kutschera, R. Naaman, M. Paul, and Z. Vager, Nucl. Instrum. Methods Phys. Res., Sect. A **281**, 663 (1989); Nucl. Instrum. Methods Phys. Res., Sect. B **52**, 378 (1990).
[25] D. Berkovits, E. Boaretto, M. Paul, and G. Hollos, Rev. Sci. Instrum. **63**, 2825 (1992).
[26] D. Berkovits, E. Boaretto, O. Heber, G. Hollos, G. Korschinek, W. Kutschera, and M. Paul, Nucl. Instrum. Methods Phys. Res., Sect. B **92**, 254 (1994).
[27] E. P. Wigner, Phys. Rev. **73**, 1002 (1948).
[28] H. Hotop and W. C. Lineberger, J. Phys. Chem. Ref. Data **14**, 731 (1985).
[29] R. R. Corderman, P. C. Engelking, and W. C. Lineberger, Appl. Phys. Lett. **36**, 533 (1980).
[30] P. A. Cox, in *Structure and Bonding,* edited by J. D. Dunitz *et al.* (Springer-Verlag, New York, 1975), Vol. 24, p. 59.
[31] R. R. Corderman, P. C. Engelking, and W. C. Lineberger, J. Chem. Phys. **70**, 4474 (1979).
[32] C. E. Moore, *Atomic Energy Levels,* Natl. Bur. Stand. (U.S.) (U.S. GPO, Washington, DC, 1952).